

21 years of Timing PSR B1509–58.

Margaret A. Livingstone ¹, Victoria M. Kaspi, Fotis P. Gavriil

Department of Physics, Rutherford Physics Building, McGill University, 3600 University Street, Montreal, Quebec, H3A 2T8, Canada

and

Richard N. Manchester

Australia National Telescope Facility, CSIRO, P.O. Box 76, Epping, NSW 1710, Australia

ABSTRACT

We present an updated timing solution for the young, energetic pulsar PSR B1509–58 based on 21.3 years of radio timing data and 7.6 years of X-ray timing data. No glitches have occurred in this time span, in contrast to other well-studied young pulsars, which show frequent glitches. We report a measurement of the third frequency derivative of $\ddot{\nu} = (-1.28 \pm 0.21) \times 10^{-31} \text{ s}^{-4}$. This value is 1.65 standard deviations from, i.e. consistent with, that predicted by the simple constant magnetic dipole model of pulsar spin-down. We measured the braking index to be $n = 2.839 \pm 0.003$ and show that it varies by 1.5% over 21.3 yr due to contamination from timing noise. Results of a low-resolution power spectral analysis of the significant noise apparent in the data yield a spectral index of $\alpha = -4.6 \pm 1.0$ for the red noise component.

Subject headings: pulsars: individual (PSR B1509–58), supernovae: individual (G320.4-1.2)

1. Introduction

Radio pulsars are powered by their rotational kinetic energy: as they emit electromagnetic radiation, their rotation rates decrease. Thus, measuring the rotational evolution of pulsars is a probe of the physics underlying these fascinating objects. Young, energetic

¹maggie@physics.mcgill.ca

pulsars, such as PSR B1509–58 are especially interesting due to their large spin-down luminosities and rapid spin-down rates. High rates of spin-down allow for the measurement of higher-order frequency derivatives, providing a deeper probe into the physics of spin-down. This slow-down can be described by

$$\dot{\nu} = -K\nu^n, \quad (1)$$

where $\nu \equiv 1/P$ is the pulse frequency, $\dot{\nu}$ is its derivative and n is the braking index. For braking by magnetic-dipole radiation in a vacuum, K is related to the dipole magnetic moment of the pulsar and $n = 3$ (Manchester & Taylor 1977). Differentiating (1) shows that n is given by

$$n = \frac{\nu\ddot{\nu}}{\dot{\nu}^2}. \quad (2)$$

The braking index is only measurable for the youngest pulsars and values not entirely dominated by noise processes have been measured for only 5 objects. In all cases, the measured values are less than the canonical value of $n = 3$ (Lyne et al. 1993; Kaspi et al. 1994a; Lyne et al. 1996; Deeter et al. 1999; Camilo et al. 2000). Implications of observed braking indices less than 3 are still being discussed (see for example, Blandford & Romani 1988) and include magnetic field growth or alignment with the spin axis, effects due to higher-order magnetic moments and the interaction of the pulsar with its relativistic particle wind.

Most pulsars do not have measurable braking indices due to a combination of contamination from low-frequency noise processes and the relatively slow spin-down of middle-aged pulsars. Because of the form of the spin-down power law given in equation 1, successive frequency derivatives go approximately as powers of the first frequency derivative. Thus most pulsars, which have values of $\dot{\nu}$ of $\sim 10^{-15} \text{ s}^{-2}$, should exhibit $\ddot{\nu}$ on the order of $\sim 10^{-30} \text{ s}^{-3}$, which would require hundreds of years of observation to measure. Many younger pulsars that could conceivably have measurable $\ddot{\nu}$ exhibit significant timing noise which masks the deterministic value of $\ddot{\nu}$ due to dipole spin-down, resulting in measured values orders of magnitude larger than predicted, often with the wrong sign. Furthermore, these values are not stable and consequently do not accurately predict pulse arrival times.

An important check on the validity of the spin-down law is the measurement of deterministic higher-order frequency derivatives. An expression for $\ddot{\nu}$ is given by taking an additional derivative of equation (1),

$$\ddot{\nu} = \frac{n(2n-1)\dot{\nu}^3}{\nu^2}. \quad (3)$$

We define the second braking index to be $m_0 \equiv n(2n-1)$. If equation 1 accurately characterizes the spin-down of the pulsar, then $m_0 = m$, where

$$m = \frac{\nu^2\ddot{\nu}}{\dot{\nu}^3}. \quad (4)$$

A measurement of m provides important insight into the spin-down of young pulsars and $m \neq m_0$ implies that the characteristic age is an under- or over- estimate of the true age, as well as having implications for a changing magnetic field (Blandford 1994). Evidently, the measurement of higher-order frequency derivatives will only be possible in the youngest pulsars that have large spin-down rates not dominated by noise processes. The Crab pulsar has a measured value of $\ddot{\nu} = (-6.45 \pm 0.02) \times 10^{-31} \text{ s}^{-4}$ (Lyne et al. 1993), in agreement with the prediction from the spin-down law, in spite of probable contamination from timing noise and frequent glitches.

PSR B1509–58 has never been observed to glitch, hence is an excellent candidate to have a measurable $\ddot{\nu}$, as well as a very accurate measurement of n . Kaspi et al. (1994a) measured a value for $\ddot{\nu} = (-1.02 \pm 0.25) \times 10^{-31} \text{ s}^{-4}$, based on 11 years of radio timing data, implying $m = 14.5 \pm 3.6$, in agreement with the predicted value $m_0 = 13.26 \pm 0.03$. The uncertainty in $\ddot{\nu}$ and thus m was known to be larger than the formal uncertainty due to contamination from significant timing noise in the data. To account, albeit not rigorously, for this effect, the quoted uncertainty is three times the formal uncertainty.

In this paper, we extend the timing analysis performed by Kaspi et al. (1994a) using an additional 10.3 yr of radio data as well as 7.6 yr of X-ray timing data to increase the precision with which the frequency evolution of PSR B1509–58 can be measured. This is accomplished by performing a phase-coherent analysis of the the data as well as a partially phase-coherent analysis that is less sensitive to the timing noise superimposed on the deterministic spin-down. In addition, we present a low-resolution spectral analysis of the timing noise and discuss possible physical causes of the noise process.

2. Observations

2.1. Radio Timing data

In our 21-yr data span, observations were made with a variety of different data acquisition instruments, at two different radio telescopes. Observations of PSR B1509–58 were conducted using the Molonglo Observatory Synthesis Telescope (MOST) at an observing frequency of 843 MHz from 1982 June 24 through 1988 June 23. Our analysis includes a total of 177 MOST pulse arrival times. For full details of these observations, see Manchester et al. (1985). All data used after 1990 were obtained using the Parkes 64-m telescope. Observations beginning 1990 March 15 and continuing at roughly monthly intervals until 21 January 1994 were described in Kaspi et al. (1994a). The same observing system, consisting of a 64-channel analog filterbank spanning 320 MHz of bandwidth at a central frequency near

1400 MHz, was used until 1997 January. Our analysis includes a total of 127 pulse arrival times obtained with the 64-channel filterbank system at Parkes. From 1997 May through 2003 October, filterbank observations were made near the same central frequency but using a 96-channel filterbank spanning 288 MHz of bandwidth. Details of this observing system, the central beam of the Parkes Multibeam receiver, can be found in Manchester et al. (2001). A total of 43 pulse arrival times were obtained with this system. Interspersed with the filterbank arrival times are data obtained also at Parkes, but using the Caltech correlator system (Navarro 1994; Sandhu et al. 1997). Typical Parkes integration times were \sim 3000 s for all systems. In spite of the variety of observing systems used, the Parkes data generally are of uniform quality, with typical folded pulse signal-to-noise ratios of \sim 20.

The Parkes data set also includes a handful of observations at a significantly higher radio frequency. These data, obtained primarily at four epochs, were used to determine the dispersion measure (DM). Two observations at 2480 MHz on 1990 March 16 were used with observations at 1400 MHz on 1990 March 15 and 1990 March 17 to determine the DM for the phase-coherent timing analysis and the DM remained constant within uncertainties throughout the entire data set (see Section 3.4). Folded pulse profiles were cross-correlated with a template to yield topocentric arrival times for each observation. Topocentric arrival times were fitted to a timing model (see Section 3.1) using the TEMPO¹ software package.

2.2. X-ray timing data

The results presented in the X-ray analysis were obtained with public data from the Proportional Counter Array (PCA; Jahoda et al. 1996) on board the Rossi X-ray Timing Explorer (*RXTE*). The PCA consists of an array of five collimated xenon/methane multi-anode proportional counter units (PCUs) operating in the 2–60 keV range, with a total effective area of approximately 6500 cm^2 and a field of view of $\sim 1^\circ$ FWHM. We used 7.6 yr of archival *RXTE* observations collected in the “GoodXenonwithPropane” mode, which records the arrival time (with $1\text{-}\mu\text{s}$ resolution) and energy (256 channel-resolution) of every unrejected xenon event as well as all the propane layer events. We used all xenon layers of each PCU in the 2–32 keV range because of the relative hardness of the source. The observations were reduced using software developed at MIT for handling raw spacecraft telemetry packet data. Data from the different PCUs were merged and binned at 1/1024 ms resolution. The data were then reduced to barycentric dynamical time (TDB) at the solar system barycenter using the known position from radio interferometry (see Table 1) and JPL DE200 solar system

¹<http://www.atnf.csiro.au/research/pulsar/tempo/>

ephemeris. Each time series was folded with 64 phase bins using the contemporaneous radio timing ephemeris. Resulting pulse profiles were cross-correlated in the Fourier domain with a high signal-to-noise-ratio template created by adding phase-aligned profiles from previous observations. We implemented a Fourier domain filter by using only the first 6 harmonics in the cross-correlation due to the relatively sinusoidal pulse profile. The cross-correlation produces an average time of arrival (TOA) for each observation.

3. Results

3.1. Phase coherent timing analysis

The stable rotation of pulsars allows (in the absence of glitches) a phase-coherent analysis of the timing data, that is, each turn of the pulsar is accounted for. This is accomplished by fitting the TOAs to a Taylor expansion of pulse phase, ϕ . Pulse phase at any time t can be expressed as

$$\phi(t) = \phi(t_0) + \nu_0(t - t_0) + \frac{1}{2}\dot{\nu}_0(t - t_0)^2 + \frac{1}{6}\ddot{\nu}_0(t - t_0)^3 + \frac{1}{24}\dddot{\nu}_0(t - t_0)^4 \dots, \quad (5)$$

where the subscript ‘0’ denotes a parameter evaluated at the reference epoch t_0 . Both the radio and X-ray TOAs were fit to the above polynomial using the software package **TEMPO**. Figure 1 shows timing residuals from a phase-coherent timing analysis with **TEMPO** with radio timing data shown as dots and X-ray data shown as crosses. The position of the pulsar was held fixed at the position determined by radio interferometry (Table 1; Gaensler et al. 1999). A constant phase offset was fitted between the radio and X-ray data to allow for the differences between the radio and X-ray pulse profiles. The top panel shows residuals with ν , $\dot{\nu}$, $\ddot{\nu}$ and $\dddot{\nu}$ fitted out. The middle panel shows the fourth frequency derivative also fitted; the bottom panel shows the residuals with the fifth frequency derivative fitted. The large concentration of power in the fifth frequency derivative is not predicted by theory, but is presumably due to timing noise. The absence of any sudden discontinuities visible in the residuals (Figure 1) indicates that no glitches have occurred in the 21.3 yr of observations.

The usual method of determining timing parameters involves fitting many higher-order derivatives to ‘pre-whiten’ the residuals (e.g. Kaspi et al. 1994b). However, we found that the value of $\dddot{\nu}$ changes with each higher-order derivative fit, without converging to a single value, and without entirely ‘whitening’ the residuals. This is due to two effects: contamination from timing noise and covariance in the fitted parameters. The value of $\dddot{\nu}$ is ambiguous from this type of analysis. A similar effect is seen with $\ddot{\nu}$, though to a much smaller level (i.e. within formal uncertainties) and is thus unimportant.

Nevertheless, it is clear from the timing residuals that there is a very significant signal from $\ddot{\nu}$ and it is unlikely that it is entirely due to timing noise. Hints that a frequency derivative may be dominated by a noise process are if the value is several orders of magnitude larger than the value predicted from theory, if it is of the wrong sign, and if it does not correctly predict pulse arrival times. None of these are true for PSR B1509–58, indicating that though there is certainly some contamination from timing noise, it is likely that the noise component does not dominate. Thus to determine $\ddot{\nu}$, we used a partially phase-coherent timing analysis as described in the next section. Spin parameters determined by the phase-coherent timing analysis are given in Table 1.

3.2. Partially phase-coherent timing analysis

To determine $\ddot{\nu}$ unambiguously, we employed a partially phase-coherent timing analysis. This method can also be used when a fully coherent solution is impossible due to glitches or large gaps in the data. We split the 21.3-yr of data into subsets of approximately 2 yr and fitted each phase-coherently. We ensured that the residuals were white for each interval and that the covariances between the fitted parameters (ν , $\dot{\nu}$ and $\ddot{\nu}$) were less than 0.9. The results are shown in Figure 2. The slope of the line, determined by a weighted least squares fit, is $\ddot{\nu}$ and has a value of $(-1.28 \pm 0.21) \times 10^{-31} \text{ s}^{-4}$. This partially coherent method heavily samples the data points at the ends of each interval, while weakly sampling the middle, so we also considered intervals that better sampled the mid-point as much as possible. We used these latter data points only to confirm the measurement of $\ddot{\nu}$, but have not included them in the quoted value because it was impossible to optimize these points in the same manner as the first set. The uncertainty was obtained from a bootstrap analysis, as we suspected that the formal uncertainty underestimated the true uncertainty due to contamination from timing noise. The bootstrap is a robust method of determining errors when a small number of sample points is available, as in this case (Efron 1979).

In addition to measuring $\ddot{\nu}$, we measured the braking index for each subset. The results are shown in Figure 3. The weighted average value is 2.839 ± 0.003 . A weighted linear least-squares fit showed that n is consistent with zero, i.e. that there is no underlying constant trend in the data. There is, however, significant variation from the average value; the reduced χ^2 is 15 for 9 degrees of freedom. This value of n is consistent with both the measurement from the fully coherent timing analysis (see Table 1) and that measured by Kaspi et al. (1994a).

3.3. Timing noise

Despite the renowned steady rotation of pulsars, there is timing noise apparent in most pulsar timing data. A low-frequency timing noise process can be seen in the residuals of PSR B1509–58 (Figure 1). These processes are typified by long-term polynomial-like trends in timing residuals after all deterministic spin-down effects have been removed. Timing noise has been shown to be correlated with \dot{P} , thus tends to be most apparent in young pulsars (Cordes & Downs 1985; Arzoumanian et al. 1994). The low-frequency nature of the noise process (giving rise to the adjective ‘red’), complicates both its removal and understanding.

One common way of characterizing timing noise is with the Δ_8 parameter, given by $\Delta_8 = \log(\frac{1}{6\nu}|\ddot{\nu}|t^3)$ (Arzoumanian et al. 1994). This parameter estimates how much the timing noise in the $\ddot{\nu}$ term contributes to the cumulative phase of the pulsar, assuming that the measurement of $\ddot{\nu}$ is *dominated by timing noise*. One must be careful when calculating the Δ_8 parameter for pulsars that have deterministic values of $\ddot{\nu}$, since these are no longer dominated by a noise process. Instead, the contribution to $\ddot{\nu}$ from timing noise must be found. We estimated the noise in this term using the partially coherent analysis explained in the previous section, by calculating the root mean square of the scatter about the deterministic trend. However, we found the uncertainty in the rms value to be larger than the rms value itself, so the value of Δ_8 is consistent with zero. This is not inconsistent with the prediction made by Arzoumanian et al. (1994), given the large amount of scatter in their data.

For a general review of timing noise in pulsars, see papers by Cordes (1980), Cordes & Helfand (1980) and Cordes & Greenstein (1981). The physical causes of timing noise in pulsars are poorly understood; possibilities range from changes in moment of inertia due to random pinning and unpinning of superfluid vortices in the core of the neutron star (Cordes & Greenstein 1981) to torques acting on the crust due to interactions between the pulsar and its magnetosphere (Cheng 1987), or that isolated pulsars may be experiencing free precession (Stairs et al. 2000).

Another possible cause of apparent timing noise in some objects is the presence of one or more planet-mass objects orbiting the neutron star. If these planets are of sufficiently low mass, their presence may appear to be ‘timing noise’ for many years. In fact, this possibility has been suggested by Rots (2002, 2004) for PSR B1509–58. He performed a fit consisting of five orbits of \sim solar mass planets to the same *RXTE* timing residuals that we have used in our analysis. To determine if these orbits were stable, we performed a periodogram analysis on both the X-ray timing residuals and the entire data set. We found roughly similar periodicities in the 7.6-yr X-ray data set, but these periodicities are not seen in the entire 21.3-yr data set. This indicates that the ‘periodicities’ are not stable in time and thus likely do not represent orbits of planets around PSR B1509–58.

3.4. Dispersion Measure Variations

One possible contributing factor to the observed timing noise is changes in the DM of the pulsar. Variations in DM have been measured for several pulsars, notably for the Crab and Vela pulsars (Backer et al. 1993; Hamilton et al. 1977). It has been postulated that the short-term DM variations observed in the Crab are due to wisps passing through the line of sight. A typical variation in DM for the Crab pulsar is $\Delta\text{DM}=0.02 \text{ pc cm}^{-3}$ with a rise time of ~ 40 days and decay time of ~ 500 days, although more recently, a DM variation of $\Delta\text{DM}=0.15 \text{ pc cm}^{-3}$ was reported (Wong et al. 2001). This caused a change in arrival time of ~ 1 ms, at an analysis frequency of 327 MHz. A similar change in DM in PSR B1509–58 would result in a change in arrival time of ~ 0.32 ms at 1400 MHz, undetectable in our data.

The DM for PSR B1509–58 was determined at four epochs where sufficient multifrequency data were obtained as shown in Table 2. Each value was determined by fitting only for ν and DM using only the multifrequency data occurring over a short time span (see Table 2). The DM was held fixed for the remainder of the timing analysis at the value obtained for the 1990 epoch. Unfortunately, any changes in the DM that occurred at epochs other than those with multifrequency data remain unmodelled and will thus contribute to the noise in the data, since the time of arrival of a pulse changes with DM.

A weighted least-squares fit was performed on the four DM measurements and the best-fit slope gives $\Delta\text{DM} = (0.42 \pm 0.19) \text{ pc cm}^{-3} \text{ yr}^{-1}$. Data spanning these four epochs were also fitted phase-coherently using **TEMPO** resulting in $\Delta\text{DM} = (0.76 \pm 0.25) \text{ pc cm}^{-3} \text{ yr}^{-1}$. Although this second measurement appears marginally significant, the small variations in observing frequency throughout the data allow timing noise to be absorbed into the ΔDM measurement, thus underestimating the uncertainties. From Table 2, we can see that the largest single change in DM (occurring between 1990 and 1996), $\sim 4 \text{ pc cm}^{-3}$, would cause a delay in arrival time of ~ 8.5 ms at 1400 MHz. There is no evidence, however, of a sudden change in DM, and a gradual change in DM of this magnitude would be difficult to detect due to the intrinsic scatter in the arrival times of the pulses.

Another determination of DM is obtained for the time period starting in 1996, when *RXTE* began observing the source. X-rays are unaffected by changes in DM, thus by comparing the X-ray and radio residuals, we can determine if changes in DM have occurred. We fit the X-ray data and all contemporaneous radio data with **TEMPO**, fitting out many higher-order derivatives to ‘pre-whiten’ the residuals. Though it is impossible to fit for DM directly with **TEMPO** between radio and X-ray data, we can compare the residuals. Due to the uncertainty between the radio and X-ray pulse profiles, we are required to fit a constant offset between the two data sets. Thus we are insensitive to any constant change in DM between this and an earlier epoch. The timing residuals show no evidence for a systematic change

in DM over 7.6 yr. However, the scatter remaining in the data is larger than expected given the TOA uncertainties. This scatter may be, in part, due to changes in DM on timescales of \sim 1-2 months, appearing random in nature in our sparsely sampled data set. The paucity of multifrequency data results in the inability to discern between short-term DM variations and a random noise process that is independent of observing frequency. We can rule out changes in DM that would change the arrival time of the pulses by more than the scatter in the data, \sim 10 ms. Thus an observing frequency of 1400 MHz, DM variations larger than 4.7 pc cm^{-3} are ruled out.

3.5. Power Spectrum Analysis

Due to the low-frequency nature of the noise process active in most pulsars, as well as the uneven sampling of our data, a traditional Fourier spectral analysis is rendered ineffective as an estimator of the power spectrum (Deeter & Boynton 1982). These problems can be partially circumvented by using a method of extracting power spectra based on orthogonal polynomials estimators developed by Groth (1975) and Deeter (1984). This method provides a low-resolution but reasonable estimate of the power contained in timing noise over a range of frequencies. To extract a power spectrum from the noise component of the timing data, the deterministic spin-down terms (in this case, ϕ , ν , $\dot{\nu}$, $\ddot{\nu}$ and $\ddot{\ddot{\nu}}$) are fit out with **TEMPO**. The next order term contains a large contribution from red noise (Figure 1), while higher-order terms will contain declining contributions from red noise and a white noise contribution attributable to measurement errors.

First, it is necessary to construct orthonormal polynomials $p_j, j = 0, 1, \dots, N$, such that

$$\sum_i p_j(t_i) p_k(t_i) = \delta_{jk}, \quad (6)$$

where each t_i represents one TOA. Due to the nature of complete sets of orthogonal polynomials, they can, given the proper coefficients, describe any function. In this case, they are used to describe the timing residuals:

$$R(t) = \sum_j c_j p_j(t), \quad (7)$$

where $R(t)$ are the residuals, and the coefficients are fitted for and described by:

$$c_j = \sum_i R(t_i) p_j(t_i). \quad (8)$$

Since ϕ , ν , $\dot{\nu}$, $\ddot{\nu}$ and $\ddot{\ddot{\nu}}$, have been already been fitted, they are completely covariant with c_0, c_1, c_2, c_3 and c_4 and thus contribute no additional information about the noise process.

Therefore c_5 is the lowest order coefficient that contains useful information about the timing noise. An estimate of the power contained at the lowest frequencies, that is $f = 1/T$, where T is the length of the data span, is given by $S_m = |c_5|^2$ (Groth 1975). It is possible to obtain further estimates of the power at higher frequencies by splitting the data into $m = 2, 4, 8, \dots$ sections, which give estimates of the power contained at $f = m/T$. For each value of m , there are m estimates of S_m , which are averaged to give the mean power estimate. Each average of S_m is distributed as a χ^2 distribution with m degrees of freedom. The averages are then corrected by a factor to account for the difference between the median and the mean of a χ^2 distribution (Kaspi et al. 1994b). The results of this analysis are plotted in Figure 4. The highest frequency term is certainly due to measurement errors, and is of the same approximate power level as the previous three terms. Thus, these terms are not included in the fit of the power spectrum. The slope obtained by fitting the three lowest frequency terms is $\alpha = -4.6 \pm 1.8$. However, fitting the fourth term, (whose uncertainty places it just above the white noise level) gives the same spectral index while better constraining the uncertainties, and implies a spectral index of $\alpha = -4.6 \pm 1.0$.

4. Discussion

4.1. Timing Analysis

The measurement of the third frequency derivative, $\ddot{\nu} = (-1.28 \pm 0.21) \times 10^{-31} \text{s}^{-4}$ is 1.65 standard deviations from the value predicted by the spin-down law. Hence the observed value and the model prediction are consistent. Typically, uncertainties on $\ddot{\nu}$ fall as t^{-4} , though the prominence of timing noise in this case will undoubtably lengthen the amount of time required. Based on the bootstrap analysis used to determine uncertainties, another $\sim 10 \text{ yr}$ of observations are required to reduce uncertainties by a factor of ~ 2 . Assuming that we have measured a stable value of $\ddot{\nu}$ and that the uncertainties will be reduced by a factor of 2, then the simple spin-down law derived assuming a constant magnetic field may not sufficiently describe the spin-down of PSR B1509–58.

The consequences of a measured $\ddot{\nu}$ different from the predicted value are most clear when comparing the measured and predicted values of the second braking index. The measured value of $\ddot{\nu}$ implies a second braking index $m = 18.3 \pm 2.9$, larger than $m_0 = 13.26 \pm 0.03$, but not significantly so given the uncertainties. Blandford (1994) discusses the implications of $m \neq m_0$, namely that K is a function of time. This discussion is particularly useful because it does not require knowledge of the true braking index, n_0 , which may be different from the measured value and cannot be predicted from theory. However, since we do not make any assumption about n_0 , we cannot say whether K is changing at the present time. A

measurement of $m \neq m_0$ does give us insight into the variation of K in the pulsar’s past. In particular, a value of $m < m_0$ implies a period of magnetic field growth early in the pulsar’s history and a true age larger than the characteristic age, while $m > m_0$ reduces the inferred age of the pulsar. Given $m - m_0 = 5.04 \pm 2.99$, and using Blandford’s prescription for the inferred age of the pulsar, the true age of PSR B1509–58 is 1000 ± 700 yr, just over half of the characteristic age, $\tau_c = 1691$ yr.

The supernova remnant (SNR) believed to be associated with PSR B1509–58 was originally estimated to have an age of 6–21 kyr (Seward et al. 1983), indicating that the pulsar’s characteristic age was underestimating the age of the system by a factor of $\sim 3.5 - 12$. However, Gaensler et al. (1999) showed that the SNR may be as young as the characteristic age of the pulsar. They show that the SNR and pulsar are interacting and explain the large size and unusual morphology of the remnant by hypothesizing that the remnant is due to an explosion of high kinetic energy or low ejected mass occurring on the edge of a cavity, thus accelerating the expansion of the remnant. At first glance, the measured value of m appears to worsen the possible age discrepancy between the pulsar and the SNR. However, the age of the remnant is clearly not well determined and could be as low as 1000 yr.

Blandford & Romani (1988) discuss the implications of a constant observed braking index, n , where in this case we must make some *a priori* assumption of the true braking index, typically assumed to be $n_0 = 3$. They give several reasons why $n < 3$ may be observed. The torque may scale with frequency differently, either due to the outflow of plasma removing a significant amount of angular momentum, or a non-dipolar magnetic field. Another interpretation of $n < 3$ is that the magnetic moment is currently varying in time, that is, $K = K(t)$. If this is the case, we can then determine a time scale for torque evolution and a check on the functional form of evolution by finding the first two dimensionless derivatives of $\dot{\nu} = -K(t)\nu^n$:

$$d_1 = n - n_0 = \frac{\dot{K}}{K} \frac{\nu}{\dot{\nu}}, \quad (9)$$

and

$$d_2 = m - n_0[2n_0 - 1 + 3(n - n_0)] = \frac{\ddot{K}}{K} \frac{\nu^2}{\dot{\nu}^2}. \quad (10)$$

Equation (9) gives a time scale for torque evolution while equation (10) provides a check for an assumed functional form for $K(t)$. For PSR B1509–58, $d_1 = -0.161 \pm 0.003$ and $d_2 = 3.5 \pm 3$. For exponential growth of K , this measurement of d_1 implies a time scale for growth of $\sim 20\,000$ yr. If the form of K is exponential we would expect that $d_2 = (d_1)^2 = 0.026$, which cannot be ruled out with the present uncertainties for d_2 . We find that the present

measurements are similarly in agreement with a power-law form for $K(t)$. The measurement of m and the large uncertainties, however, are consistent with the simplest explanation of a constant value of K and thus a constant magnetic field.

Despite scatter due to timing noise, the braking index is constant over 21.3 yr to within 1.5%. This result is similar to that of the Crab pulsar's braking index, reported to be constant to within 0.5%, where measurements were obtained between glitch events and are typically based on five years of data (Lyne et al. 1993). This reinforces the need for long-term timing to measure the true value of braking indices to such precision.

4.2. Timing noise analysis

4.2.1. Glitches

Our phase-coherent analysis shows that, due to the absence of any sudden discontinuities in the timing residuals, PSR B1509–58 has not glitched in 21.3 yr. PSR B1509–58 is the only young pulsar known that has never glitched over a long period of time. Lyne (1999) showed that there is a correlation not only between \dot{P} and timing noise, but \dot{P} and glitch activity, although some of the youngest pulsars (i.e. the Crab) have glitch activity parameters smaller than expected from the correlation. The explanation for this is that the internal temperature of the youngest pulsars is too high for large scale vortex pinning and unpinning. If this is the case, then the fact that PSR B1509–58 has the lowest glitch rate among young pulsars would suggest that it has the highest internal temperature, in spite its characteristic age being larger than that of the Crab pulsar. On the other hand, so-called ‘anomalous X-ray pulsars’ (AXPs) have been observed to glitch with parameters that are not very different from those seen in radio pulsars (Kaspi et al. 2000; Kaspi & Gavriil 2003; Dall’Osso et al. 2003). Given their estimated surface temperatures and luminosities (measured via X-ray spectral observations) AXPs appear to be much hotter than any known radio pulsar. If AXP glitches indeed have the same physical origin as do glitches in rotation-powered pulsars, this argues that the glitch phenomenon is not strongly affected by neutron-star temperature.

4.2.2. Spectral Analysis

The spectral index for the timing noise of PSR B1509–58, $\alpha = -4.6 \pm 1.0$ is marginally steeper than that measured for other pulsars. The low-resolution nature of the Deeter method, however, provides only a rough estimate of the true spectral index of the noise. The spectral index of the timing noise for the Crab pulsar has been determined several times,

the most recent of which found $\alpha = -3$ as well as a periodic component with period of 568 ± 10 days (Scott et al. 2003), using a modified Fourier analysis (possible in this case due to the dense sampling of the Crab timing data from 1982-1989). The spectral index was then verified with the Deeter polynomial method, though this analysis does not probe the lowest frequencies (i.e. longest timescales) available. Previous analyses of Crab timing data were consistent with $\alpha \sim -4$ (Deeter 1981; Cordes 1980). Cordes & Helfand (1980) show that the timing noise of 11 pulsars is consistent with a pure random walk in phase, frequency or frequency derivative. However, D’Alessandro et al. (1995) show in a study of 45 pulsars that only 5 are consistent with a pure random walk, while most pulsars exhibit timing noise either due to a combination of a random walk and discrete jumps, or inconsistent with either hypothesis. Other pulsars have been shown to have spectral indices of timing noise ranging from $\alpha \sim -0.5$ to -2.4 (Baykal et al. 1999). Thus there is a range of possible spectral indices that describe timing noise in different pulsars.

Although there is no physical reason why the spectral index must be an even integer, these are the only cases for which analytical solutions exist. For PSR B1509–58, the measured spectral index is consistent with having a component of frequency noise, that is, a random walk in pulse frequency corresponding to $\alpha = -4$. The measured value of the spectral index indicates that there may also be a component due to a random walk in frequency derivative, characterized by $\alpha = -6$. Although the measured spectral index alone would seem to indicate a random walk in frequency, the fact that the residuals are not Gaussian distributed after fitting for higher derivatives indicates that this is not the case. A random walk in the k th derivative of phase is mathematically equivalent to a white noise process in the $(k+1)$ derivative (Groth 1975). This should correspond to ‘white’ residuals after fitting out the $(k+1)$ derivative, not seen in the timing residuals of PSR B1509–58.

One of the problems in quantifying timing noise is the lack of a comprehensive theory of its physical causes. In fact it is possible that there are several causes of timing noise active in one object, thus complicating the interpretation of the measured spectral index. Free precession is an interesting solution to the timing noise problem because it can be detected from the changes in the pulse profile as well as a periodicity in the timing residuals (Stairs et al. 2000). Unfortunately, the data quality and lack of a long baseline for many pulsars prohibits the discovery of this process. If undetected, precession would contribute to the apparent timing noise of the pulsar and the spectral index of the noise, despite the fact that it is not a random process. Additionally, other physical causes of noise, (e.g. magnetospheric torques or random vortex pinning and unpinning) will contribute to the measured spectral index.

Another common problem in assessing the cause of timing noise is that quasi-periodicities

are apparent in the timing residuals of most pulsars. An artificial quasi-periodicity will change with the length of the data set, while a real quasi-periodicity will not (Konacki et al. 1999). To begin to truly understand timing noise in pulsars, it is crucial that new high-resolution spectral methods, capable of discerning discrete features due to periodicities, are developed. New methods must be able to deal with both the spectral leakage and data sampling problems that presently constrain our measurements and thus understanding of timing noise. Another problem in developing high-resolution methods for very long period noise is the extremely long time baselines required to observe many periods of the noise; the only way to solve this is by brute force, that is, by timing pulsars for hundreds of years. A better understanding, both mathematically and physically, of timing noise will allow for a better understanding of the deterministic spin-down of pulsars underlying the noise processes.

The authors gratefully acknowledge A. Atoyan, S.M. Ransom and M.S.E. Roberts for helpful discussions on topics relating to this research. The Molonglo Radio Observatory is operated by the University of Sydney. The Parkes radio telescope is part of the Australia Telescope which is funded by the Commonwealth of Australia for operation as a National Facility managed by CSIRO. This research made use of data obtained from the High Energy Astrophysics Science Archive Research Center Online Service, provided by the NASA-Goddard Space Flight Center. VMK is a Canada Research Chair and an NSERC Steacie Fellow. Funding for this work was provided by NSERC Discovery Grant Rgpip 228738-03 and Steacie Supplement Smfsu 268264-03. Additional funding came from Fonds de recherche de la nature et des technologies du Quebec (NATEQ), the Canadian Institute for Advanced Research, and the Canada Foundation for Innovation.

REFERENCES

Arzoumanian, Z., Nice, D. J., Taylor, J. H., & Thorsett, S. E. 1994, *ApJ*, 422, 671

Backer, D. C., Hama, S., Van Hook, S., & Foster, R. S. 1993, *ApJ*, 404, 636

Baykal, A., Ali Alpar, M., Boynton, P., & Deeter, J. 1999, *MNRAS*, 306, 207

Blandford, R. D. 1994, *MNRAS*, 267, L7

Blandford, R. D. & Romani, R. W. 1988, *MNRAS*, 234, 57P

Camilo, F., Kaspi, V. M., Lyne, A. G., Manchester, R. N., Bell, J. F., D'Amico, N., McKay, N. P. F., & Crawford, F. 2000, *ApJ*, 541, 367

Cheng, K. S. 1987, *ApJ*, 321, 799

Cordes, J. M. 1980, *ApJ*, 237, 216

Cordes, J. M. & Downs, G. S. 1985, *ApJS*, 59, 343

Cordes, J. M. & Greenstein, G. 1981, *ApJ*, 245, 1060

Cordes, J. M. & Helfand, D. J. 1980, *ApJ*, 239, 640

D'Alessandro, F., McCulloch, P. M., Hamilton, P. A., & Deshpande, A. A. 1995, *MNRAS*, 277, 1033

Dall'Osso, S., Israel, G. L., Stella, L., Possenti, A., & Perozzi, E. 2003, *ApJ*, 599, 485

Deeter, J. 1984, *ApJ*, 281, 482

Deeter, J. E. 1981, Ph.D. Thesis

Deeter, J. E. & Boynton, P. E. 1982, *ApJ*, 261, 337

Deeter, J. E., Nagase, F., & Boynton, P. E. 1999, *ApJ*, 512, 300

Efron, B. 1979, *The Annals of Statistics*, 7, 1

Gaensler, B. M., Brazier, K. T. S., Manchester, R. N., Johnston, S., & Green, A. J. 1999, *MNRAS*, 305, 724

Groth, E. J. 1975, *ApJS*, 29, 431

Hamilton, P. A., McCulloch, P. M., Manchester, R. N., Ables, J. G., & Komesaroff, M. M. 1977, *Nature*, 265, 224

Jahoda, K., Swank, J. H., Giles, A. B., Stark, M. J., Strohmayer, T., Zhang, W., & Morgan, E. H. 1996, *2808*, 59

Kaspi, V. M. & Gavriil, F. P. 2003, *ApJ*, 596, L71

Kaspi, V. M., Lackey, J. R., & Chakrabarty, D. 2000, *ApJ*, 537, L31

Kaspi, V. M., Manchester, R. N., Siegman, B., Johnston, S., & Lyne, A. G. 1994a, *ApJ*, 422, L83

Kaspi, V. M., Taylor, J. H., & Ryba, M. 1994b, *ApJ*, 428, 713

Konacki, M., Lewandowski, W., Wolszczan, A., Doroshenko, O., & Kramer, M. 1999, *ApJ*, 519, L81

Lyne, A. 1999, in Pulsar Timing, General Relativity and the Internal Structure of Neutron Stars, 141–+

Lyne, A. G., Pritchard, R. S., Graham-Smith, F., & Camilo, F. 1996, *Nature*, 381, 497

Lyne, A. G., Pritchard, R. S., & Smith, F. G. 1993, *MNRAS*, 265, 1003

Manchester, R. N., Durdin, J. M., & Newton, L. M. 1985, *Nature*, 313, 374

Manchester, R. N., Lyne, A. G., Camilo, F., Bell, J. F., Kaspi, V. M., D’Amico, N., McKay, N. P. F., Crawford, F., Stairs, I. H., Possenti, A., Morris, D. J., & Sheppard, D. C. 2001, *MNRAS*, 328, 17

Manchester, R. N. & Taylor, J. H. 1977, *Pulsars* (San Francisco: Freeman)

Navarro, J. 1994, PhD thesis, California Institute of Technology

Rots, A. 2002, *APS Meeting Abstracts*, 17028

Rots, A. 2004, in *X-ray Timing 2003: Rossi and Beyond*, ed. F. L. P. Kaaret & J. Swank (Melville, NY: American Institute of Physics)

Sandhu, J. S., Bailes, M., Manchester, R. N., Navarro, J., Kulkarni, S. R., & Anderson, S. B. 1997, *ApJ*, 478, L95

Scott, D., Finger, M., & Wilson, C. 2003, *MNRAS*, 344, 412

Seward, F. D., Harnden Jr., F. R., Murdin, P., & Clark, D. H. 1983, *ApJ*, 267, 698

Stairs, I. H., Lyne, A. G., & Shemar, S. L. 2000, *Nature*, 406, 484

Wong, T., Backer, D. C., & Lyne, A. 2001, *ApJ*, 548, 447

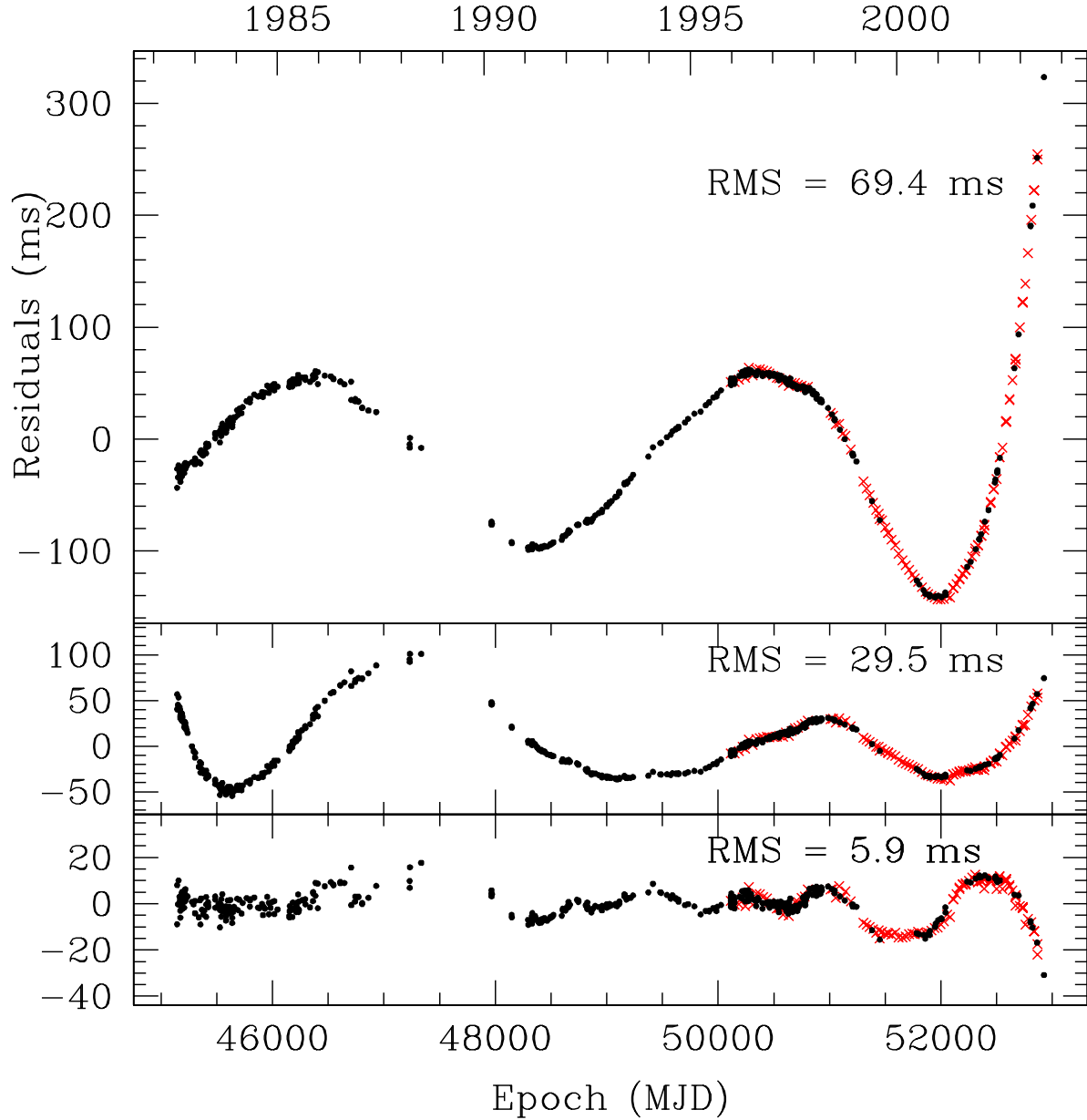


Fig. 1.— Timing residuals for PSR B1509–58. Radio TOAs are shown as dots; the X-ray TOAs as crosses. The top panel has a quartic polynomial (i.e. $\ddot{\nu}$), removed, the middle panel has a quintic removed and the bottom panel shows the residuals after the removal of a sixth degree polynomial. See the electronic edition of the Journal for a colour version of this figure.

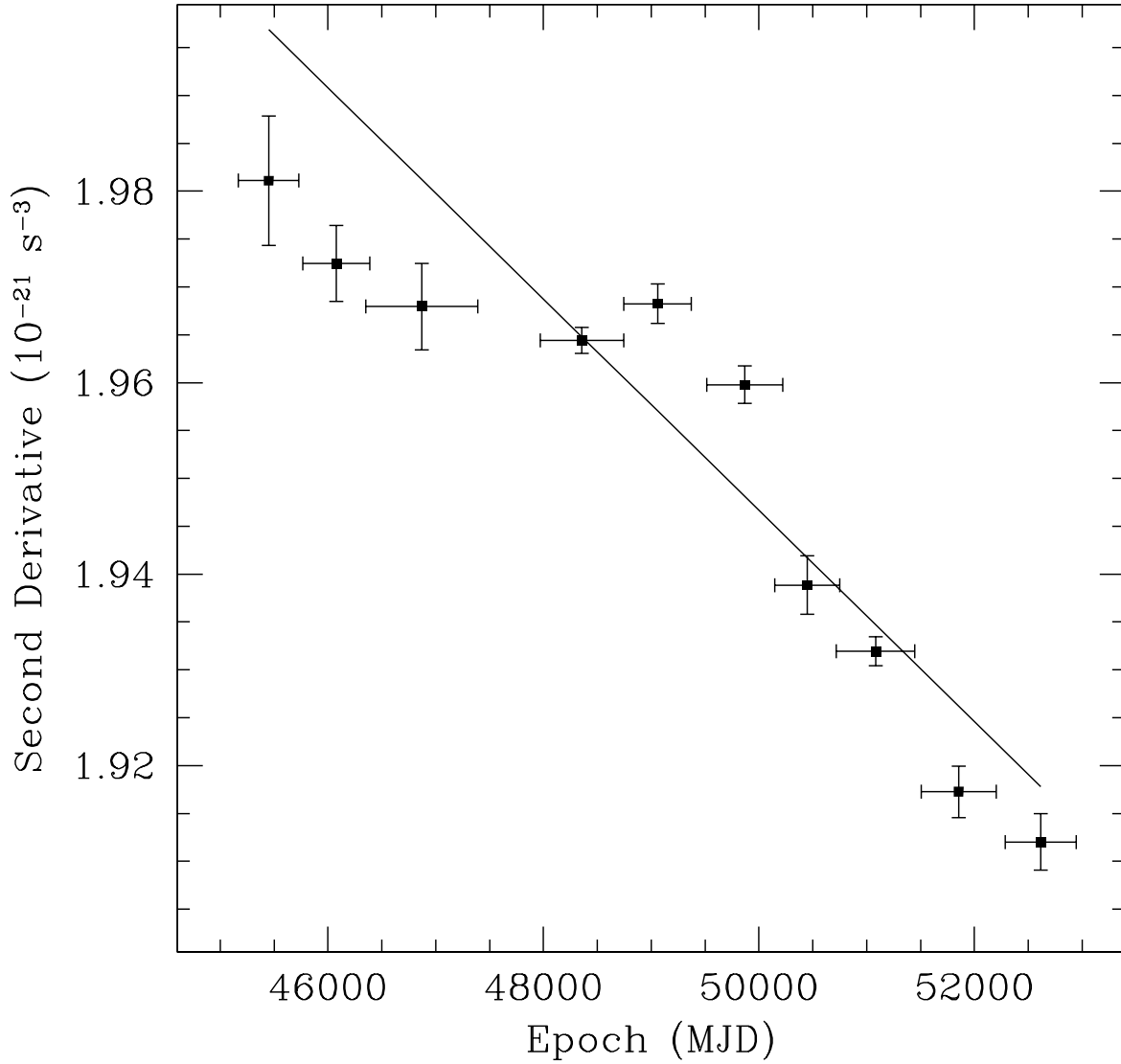


Fig. 2.— Second derivative of pulse frequency from phase-coherent subsets versus epoch. The slope of the line is $\ddot{\nu}$ and has a value of $(-1.28 \pm 0.21) \times 10^{-31} \text{ s}^{-4}$.

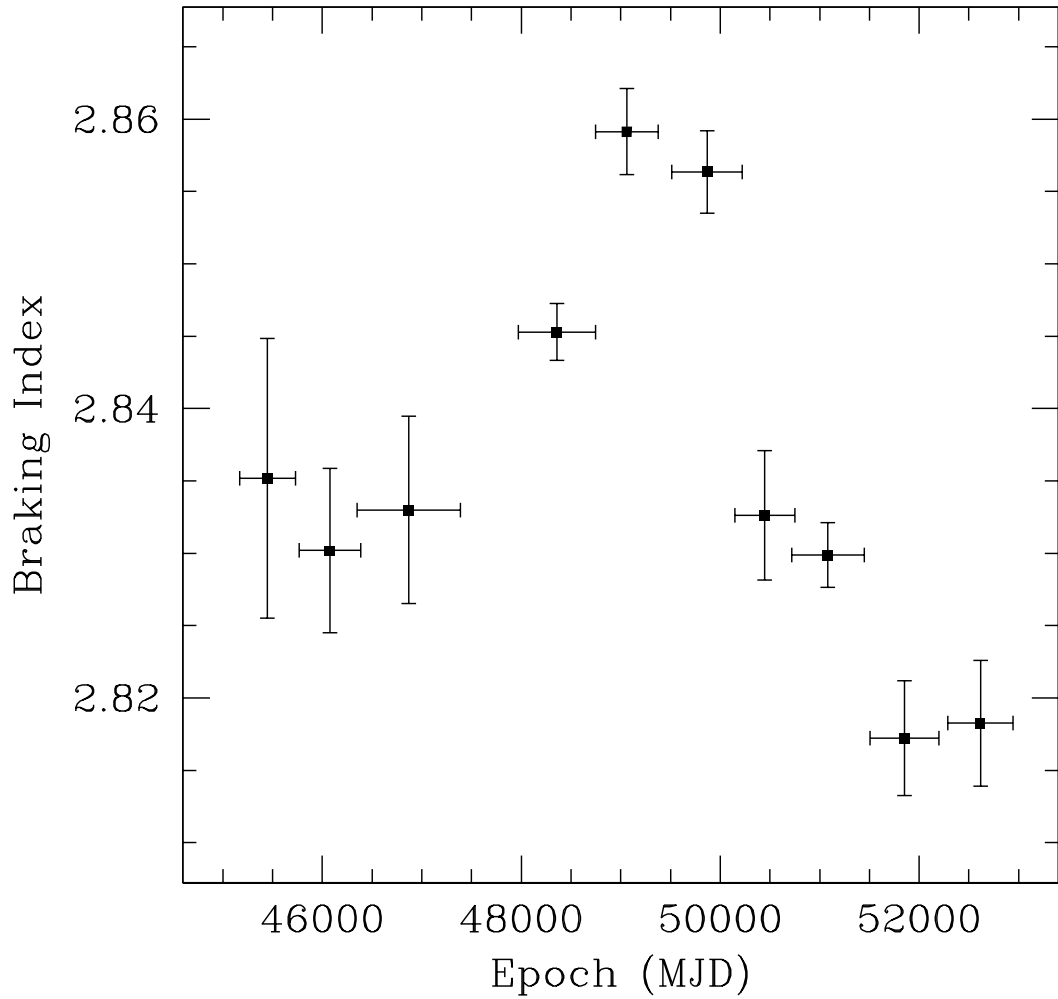


Fig. 3.— Braking index calculated at each epoch. There is no statistically significant change over 21.3 years of data. The average value is 2.839 ± 0.003 , in agreement with the previously reported value (Kaspi et al. 1994a) and the value obtained in a fully phase-coherent analysis (Table 1). The reduced χ^2 value is 15 for 9 degrees of freedom, suggesting contamination by timing noise (see Section 3.2).

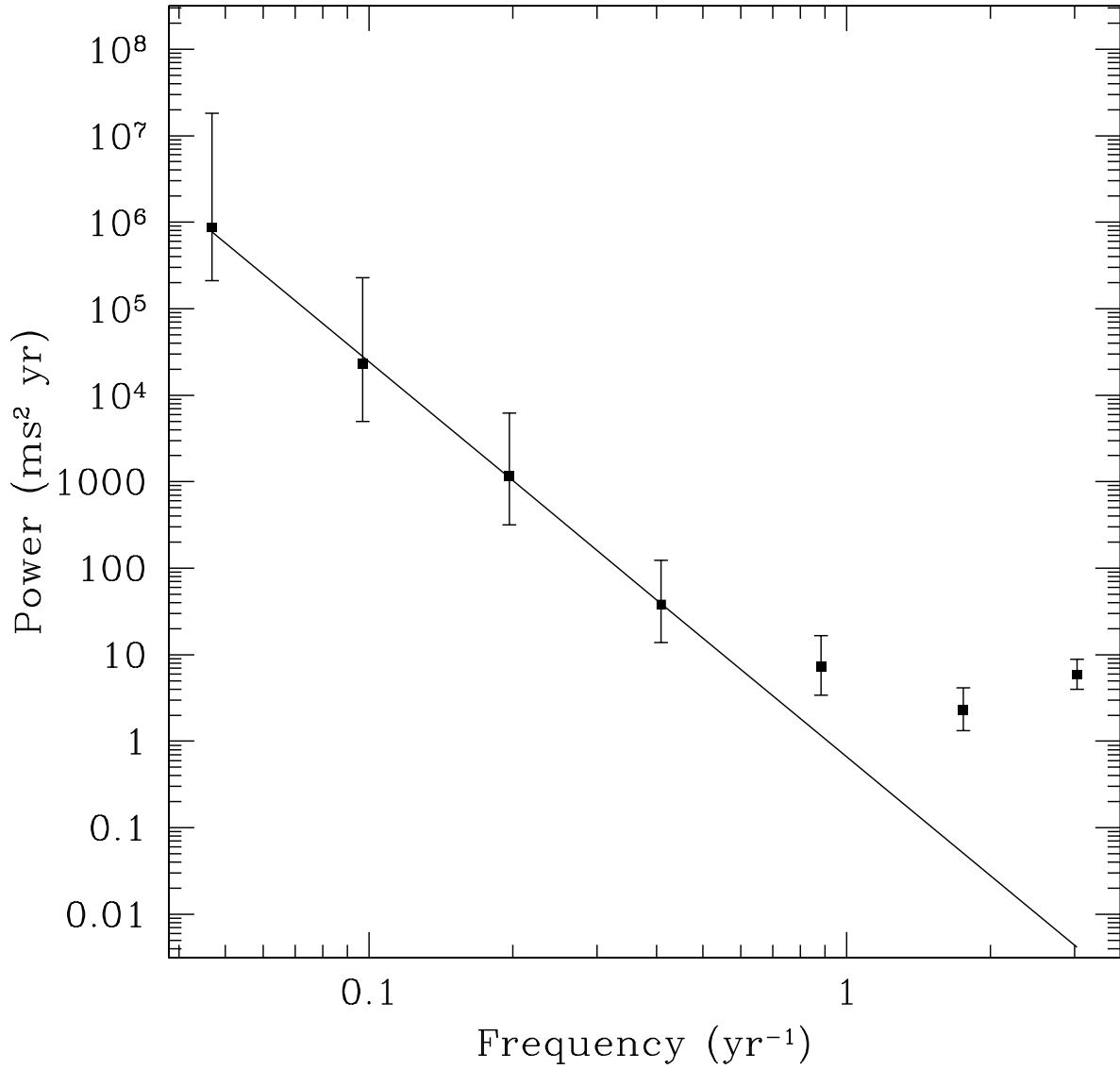


Fig. 4.— Power spectrum of the timing noise exhibited by PSR B1509–58. The best-fit line gives a spectral index of $\alpha = -4.6 \pm 1.0$. The last three points are dominated by measurement errors, thus are not fit as part of the red noise spectrum.

Table 1. Parameters for PSR B1509–58.

Parameters for phase-coherent analysis.	
Dates (Modified Julian Day)	45114 - 52925
Epoch (Modified Julian Day)	49034.5
Right Ascension ^a (J2000)	15h 13m 55.62s
Declination ^a (J2000)	–59°08'09.0"
ν (Hz)	6.633598804(3)
$\dot{\nu}$ (10^{-11} s $^{-2}$)	–6.75801754(4)
$\ddot{\nu}$ (10^{-21} s $^{-3}$)	1.95671(2)
Braking Index, n	2.84209(3)
Dispersion Measure ^a (pc cm $^{-3}$)	253.2

Parameters for partially coherent analysis.	
Braking Index, n	2.839(3)
$\ddot{\nu}$ (10^{-31} s $^{-4}$)	–1.28(21)
Second braking index, m	18.3(2.9)

^aHeld fixed for phase-coherent analysis.

Table 2. Dispersion Measure at four epochs.

Epoch	DM (pc cm $^{-3}$)
March 15 1990	253.2±1.9
February 1 - February 4 1996	257.4±1.2
February 29 - March 1 1996	255.5±0.9
January 12 - January 14 1997	254.8±1.1